

Design and performance of solar powered absorption cooling systems in office buildings

Ursula Eicker, Dirk Pietruschka

University of Applied Sciences Stuttgart, Schellingstrasse 24, D-70174 Stuttgart,

Tel +49 711 8926 2831, Fax +49 711 8926 2698, Email: ursula.eicker@hft-stuttgart.de

Published in Energy and Buildings (2009), Volume 41, Issue 1, January 2009, Pages 81-91

Abstract

The paper contributes to the system design of solar thermal absorption chillers. A full simulation model was developed for absorption cooling systems, combined with a stratified storage tank, steady state or dynamic collector model and hourly resolved building loads. The model was validated with experimental data from various solar cooling plants.

As the absorption chillers can be operated at reduced generator temperatures under partial load conditions, the control strategy has a strong influence on the solar thermal system design and performance. It could be shown that buildings with the same maximum cooling load, but very different load time series, require collector areas varying by more than a factor 2 to achieve the same solar fraction. Depending on control strategy, recooling temperature levels, location and cooling load time series, between 1.7 and 3.6 m² vacuum tube collectors per kW cooling load are required to cover 80% of the cooling load.

The cost analysis shows that Southern European locations with higher cooling energy demand lead to significantly lower costs. For long operation hours, cooling costs are around 200 € MWh⁻¹ and about 280 € MWh⁻¹ for buildings with lower internal gains and shorter cooling periods. For a Southern German climate, the costs are more than double.

Introduction

Solar or waste heat driven absorption cooling plants can provide summer comfort conditions in buildings at low primary energy consumption. For the often used single effect machines, the ratio of cold production to input heat (COP) is in the range of 0.5 – 0.8, while electrically driven compression chillers today work at COPs around 3.0 or higher. Solar fractions therefore need to be higher than about 50% to start saving primary energy (Mendes et al, 1998). The exact value of the minimum solar fraction required for energy saving not only depends on the performance of the thermal chiller, but also on other components such as the cooling tower: a thermal cooling system with an energy efficient cooling tower performs better than a compression chiller at a solar fraction of 40%, a low efficiency cooling tower increases the required solar fraction to 63%. These values were calculated for a thermal chiller COP of 0.7, a compressor COP of 2.5 and an electricity consumption of the cooling tower between 0.02 or 0.08 kWh_{el} per kWh of cold (Henning, 2004).

Double effect absorption cycles have considerably higher COPs around 1.1 – 1.4, but require significantly higher driving temperatures between 120 and 170°C (Wardono and Nelson, 1996), so that the energetical and economical performance of the solar thermal cooling system is not necessarily better (Grossmann, 2002).

Several authors published detailed analyses of the absorption cycle performance for different boundary conditions, which showed the very strong influence of cooling water temperature, but also of chilled water and generator driving temperature levels on the coefficient of performance (Engler et al, 1997, Kim et al, 2002). Most models resolve the internal steady state energy and mass balances in the machines and derive the internal temperature levels from the applied external temperatures and heat transfer coefficients of the evaporator, absorber, generator and condenser heat exchangers. To simplify the performance calculations, characteristic equations have been developed (Ziegler, 1998), which are an exact solution of the internal energy balances for one given design point and which are then used as a simple linear equation for different boundary conditions. For larger deviations from design conditions or for absorption chillers with thermally driven bubble pumps, one single equation does not reproduce accurately the chiller performance (Albers and Ziegler, 2003). The disadvantages of the characteristic equation can be easily overcome, if dynamic simulation tools are used for the performance analysis

and internal enthalpies are calculated at each time step – an approach, which is chosen in this paper using the simulation environment INSEL (Schumacher, 1991).

Dynamic models taking into account the thermal mass of the chillers are also available and can be used for the detailed optimisation of control strategies such as machine start up (Kim et al, 2003, Willers et al, 1999). However, for an energetic analysis of annual system performance, steady state models are sufficiently accurate.

The available steady state models of the absorption chillers provide a good basis for planners to dimension the cooling system with its periphery such as fans and pumps, but they do not give any hint for the dimensioning of the solar collectors or any indication of the solar thermal contribution to total energy requirements. This annual system performance depends on the details of the collector, storage and absorption chiller dimensions and efficiencies for the varying control strategies and building load conditions. An analysis of the primary energy savings for a given configuration with renewable energy heat input requires a complete model of the cooling system coupled to the building load with a time resolution of at least one hour.

Very few results of complete system simulations have been published. In the IEA task 25 several design methods have been evaluated. In the simplest approach a building load file provides hourly values of cooling loads and the solar fraction is calculated from the hourly produced collector energy at the given irradiance conditions. Excess energy from the collector can be stored in completely mixed buffer volumes. Different building types were compared for a range of climatic conditions in Europe with cooling energy demands between 10 – 100 kWh m⁻²a⁻¹. Collector surfaces between 0.2 – 0.3 m² per square meter of conditioned building space combined with 1 – 2 kWh of storage energy gave solar fractions above 70% (Henning, 2004).

System simulations for an 11 kW absorption chiller using the dynamic simulation tool TRNSYS gave an optimum collector surface of only 15 m² for a building with 196 m² surface and 90 kWh m⁻² annual cooling load, i.e. less than 0.1 m² per square meter of building surface. A storage volume of 0.6 m³ was found to be optimum (40 liter per m² collector), which at 20K useful temperature level only corresponds to 14 kWh or 0.07 kWh per square meter of building surface (Florides et al, 2002). Another system simulation study (Atmaca et al, 2003) considered a constant cooling load of 10.5 kW and a collector field of 50 m². 75 liters storage volume per square meter of collector surface were found to be optimum. Larger storage volumes were detrimental to performance.

The main limitations of these models are that the absorption chillers are not simulated with varying driving temperature levels and that the storage models only balance energy flows, but do not consider stratification of temperatures. This explains the performance decrease with increasing buffer volume, if the whole buffer volume has to be heated up to reach the required generator temperatures.

Also attempts have been made to relate the installed collector surface to the installed nominal cooling power of the chillers in real project installations. The surface areas varied between 0.5 and 5 m² per kW of cooling power with an average of 2.5 m² kW⁻¹. To summarize the available solar cooling simulation literature, there are detailed thermal chiller models available, which are mainly used for chiller optimisation and design and not for yearly system simulation. Solar thermal systems on the other hand, have been dynamically modelled mainly for heating applications. Accurate coupled models of chillers, solar thermal systems and building loads are the focus of the current work. The simulation work is based on hourly time series of irradiance and temperature data for the two locations Madrid in Spain and Stuttgart in Germany. The hourly time series have been generated using long term monthly averages of both global horizontal irradiance and temperature, which are available for example in the database of the INSEL simulation environment. Using the monthly mean values, the well validated algorithms of Gordon and Reddy were used to first statistically generate daily clearness indices, which are not normally distributed around the monthly mean value. The hourly irradiance time series is then obtained by a first order autoregressive procedure, which uses a model from Collares-Pereira to parameterize the hourly clearness index.

Scope and methodology of the work

The paper analyses the energetic and economical performance of solar powered absorption chiller systems. The goals are to calculate the solar contribution to the total energy demand of the thermal chiller system and to specify the associated costs. The influence of the building type and different cooling load distributions on dimensioning rules was the main question of the work.

To evaluate the influence of chiller and solar thermal system sizing on performance, cooling load files for a small office building with about 450 m² surface area were produced to fit a commercially available absorption chiller with 15 kW nominal cooling power available on the German market (EAW, 2003). The building window surface area and orientation, the shading system and the internal loads were varied to determine the influences of the load distribution on solar fraction.

The building construction (insulation standards, orientation, glazing fraction, size etc.) was chosen so that a given chiller power is sufficient to maintain room temperature levels at a given setpoint of 24°C for at least 90% of all occupation hours. To evaluate the influence of the time dependent building cooling loads on the solar fraction, building load files were calculated with a dominance of internal loads through persons or equipment or with dominating external loads through glazed facades.

For the economical analysis, a market survey of thermal chillers up to 200 kW cooling power and for solar thermal collector systems was carried out. The annuity was calculated for different system combinations and cooling energy costs were obtained.

Component and system models and experimental validation

Absorption chiller models

Steady state absorption chiller models are based on the internal mass and energy balances in all components, which depend on the solution pump flow rate and on the heat transfer between external and internal temperature levels. Several problems are associated with a single characteristic equation, which calculates all internal enthalpies only for the design conditions: if bubble pumps are used, the solution flow rate strongly depends on the generator temperature. Also if the external temperature levels differ significantly from design conditions, the internal temperature levels change and consequently the enthalpies. Therefore, in the current work, the internal energy balances were solved for each simulation time step as a function of the external entrance temperatures, so that changing mass flow rates can be considered in the model.

For a given cold water temperature, the cooling power and the COP mainly depend on the generator and the cooling water temperatures for the absorption and condensation process. If the temperatures deviate significantly from the design point, the variable enthalpy model reproduces the measured results much better than the constant enthalpy equation. This is shown in figure 1 for a new 10 kW LiBr – H₂O machine produced by the German company Phoenix, where the slopes for both evaporator cooling power and COP are better met at low and high generator temperatures. The design generator entry temperature is 75°C at an absorber cooling water entry temperature of 27°C and an evaporator temperature of 18°C.

At lower evaporator temperatures, the COP is lower and the generator temperature has to be increased. This shown for a 15 kW LiBr – H₂O machine produced by the German company EAW with a design generator entry temperature of 90°C at an absorber cooling water entry temperature of 27°C and an evaporator entry temperature of 12°C and exit of 6°C (see figure 2).

The cooling water temperature has a strong influence on cooling power delivered (see figure 3). To compare performance of different absorption chillers, it is therefore essential to compare for the same three temperature levels of evaporator, absorber/condensor and generator.

As the absorption chiller model is part of a more complex dynamic model including varying meteorological conditions, there is a need to use dynamic system simulation tools anyway. The simplification of the easy to use characteristic equation with constant slopes is therefore not advantageous and the more exact quasi – stationary model has been used throughout this work.

Building cooling load characteristics

To evaluate the energetic and economic performance of solar cooling systems under varying conditions, different building cooling load files were produced with the simulation tool TRNSYS. The methodology for choosing the building shell parameters is as follows: For a given chiller power of 15 kW an adequate building size was selected, for example a south orientated office building with 425 m² surface area and of rectangular geometry. The orientation of the building was varied to study the influence of daily fluctuations of external loads. The dimensions and window opening of the buildings were adjusted, so

that the given chiller power could keep the temperature levels below a setpoint of 24°C for more than 90% of all operation hours.

The air exchange rates were held constant at 0.3 h⁻¹ for the office throughout the year. This limited air exchange rate leads to cooling load files, which in some cases contain cooling power demand during winter and transition periods for southern European locations. Only if the air exchange rate can be significantly increased either by natural ventilation or by using a mechanical ventilation system, can such a cooling power demand be reduced by free cooling. In the buildings analysed in this work, heat was always removed by a water based distribution system, which was fed by cold water from the cooling machines. At low ambient temperatures, the cooling tower alone provides the required temperature levels for the cold distribution system.

To evaluate the influence of the specific time series of the building cooling load, two cases were simulated:

- Case 1: Cooling load dominated by external loads through solar irradiance for unshaded windows and low internal loads of 4 W m⁻² (see figure 5).
- Case 2: Cooling load dominated by internal loads of 20 W m⁻² with good sun protection of all windows (see figure 7 and table 2).

In addition, case 1a is an office building with the same geometry, but the main window front to the east instead of south. Case 1b has nearly 40% of the windows facing west. The peak values of the daily cooling loads are highest for the office with a western window front and lowest for the eastern offices. The phase shift between the curves is about one hour (see figure 4).

The cooling load file with high internal loads shows less daily fluctuations and is dominated by the external temperature conditions. For the office building, the load is between 12 – 14 MWh for low internal loads up to 30 MWh for the same building, but higher internal loads. The same building at a different geographical location (Stuttgart in Germany instead of Madrid in Spain) has a cooling energy demand of only 4.7 MWh. A wide range of specific cooling energies is covered, ranging from about 10 kWh m⁻² for an office with low internal loads in a moderate climate up to 70 kWh m⁻² for the same building in Madrid and high internal loads (figure 8).

The specifications for the buildings with the different cases are summarized in tables 1 and 2.

A crucial factor for the economics of the solar cooling installations are the operation hours of the machines, whereby buildings with higher full load operation have lower cooling costs for the investment part. The load hours for the buildings considered are between 680 and 2370 for the location Madrid and only 313 for an office building in Stuttgart (table 3).

Solar thermal system models

The solar thermal system model includes a collector, a stratified storage tank, a controller and a back-up heater. The thermal collector is simulated using the steady state collector equation with an optical efficiency $\eta_0 F'$ and the two linear and quadratic heat loss coefficients U_{L1} and U_{L2} . A vacuum tube collector from the company Schott was used for all simulation runs and has an optical efficiency of 0.775, with U_{L1} at 1.476 W m⁻²K⁻¹ and U_{L2} at 0.0075 W m⁻²K⁻². The storage tank has 10 temperature nodes to simulate stratification. The collector injects heat into the storage tank via a plate heat exchanger, if the collector temperature is 5 K above the lowest storage tank temperature. The return to the collector is always taken from the bottom of the tank, the load supply is taken from the top of the tank. The collector outlet and the load return is put into the storage tank at the corresponding stratification temperature level. To validate the collector model using experimental data, a dynamic model was also developed, which includes heat capacity effects. However, for the yearly simulation, the steady state model was considered as sufficiently accurate.

System simulation results

General influences of thermal system component design

Before evaluating the influence of the building cooling load, the thermal cooling system performance was studied in detail for one chosen load file, namely the office building dominated by external loads

(office 1). The main influences on the cooling system performance are the external temperature levels in the generator, evaporator, absorber and condenser. In case of the evaporator, the temperature level depends on the type of cold distribution system, for example fan coils with 6°C/12°C or chilled or activated ceilings with higher temperature levels of 15°C/21°C. The higher the temperature of the cold distribution, the better the system performance. In case of the absorber and condenser temperature levels, the type and control of the recooling system is decisive for performance. In this work, wet and dry cooling towers have been modelled. The generator temperature level mainly depends on the chosen control strategy. In the simplest case, the inlet temperature to the generator is fixed, which means high collector temperatures and poorer performance. An improved control strategy allows a temperature reduction in partial load conditions.

For an annual cooling energy demand of nearly 14 MWh and an average COP of 0.7 the system requires about 20 MWh of heating energy. To achieve a solar fraction of 80% for the given cooling load profile, a collector surface area of 48.5 m² and a storage tank volume of 2 m³ is required, if the generator is always operated at an inlet temperature of 85°C. For the constant generator inlet temperature level of 85°C, the specific collector energy yield is only 393 kWh m⁻²a⁻¹ for an annual irradiance of 1746 kWh m⁻²a⁻¹, i.e. the solar thermal system efficiency is 22% (Case 0). If the collector field would also be used for warm water heating and heating support the annual yield could be significantly increased (to about 1000 kWh m⁻²a⁻¹).

For such constant high generator inlet temperatures and a low flow collector system with 15 kg⁻¹ m⁻² h⁻¹ mass flow, the temperature levels in the collector are often above 100°C, if the cooling demand is low and the solar thermal energy production high. An increase of mass flow reduces the problem: by doubling the collector mass flow and thus lowering average solar collector temperatures, the solar fraction for the same collector surface area rises to 90% (see figure 9). Using the higher mass flow of 30 kg m⁻² h⁻¹ and constant generator temperatures, the collector surface area can be reduced to 33.1 m² and the collector energy yield rises to 584 kWh m⁻² a⁻¹ (Case 1).

If the controller allows a reduction of generator temperature for partial load conditions, performance improves due to lower average temperature levels and low flow systems can again be used (see figure 10). The collector surface area required to cover 80% of the demand is now reduced to 31 m², i.e. only 2 m² kW⁻¹. The cold water temperatures were still at 12°C/6°C and a wet cooling tower was used (Case 2).

If the cold is distributed using chilled ceilings or thermally activated concrete slabs, the temperature levels can be raised and performance improves (Case 3). For cold water temperatures of 21°C/15°C the required collector surface area is only 27 m², i.e. 1.8 m² kW⁻¹ (see figure 11).

If a dry cooling tower is used, the heat removal of absorber and condenser occurs above ambient air temperature levels (Case 4). The setpoint for the absorber inlet temperature is 27°C, which cannot always be reached for the dry cooling tower. This leads to an increase of required collector surface area to 36 m², i.e. 2.4 m² kW⁻¹. The cases are summarized in table 4.

For the improved control strategy, the collector energy delivered to the storage tank reaches between 511 and 670 kWh m⁻²a⁻¹ depending on the cold and recooling water temperature levels.

The thermal COP of the absorption chiller is highest (0.76), if the cold water temperature level is high (21°C/15°C) and stays high, even if a dry recoler is used (0.73). Low cold water temperature give COP's of 0.67 – 0.7 (see figure 12). The solar thermal efficiency is calculated from the energy produced and delivered to the hot storage tank divided by the solar irradiance.

The storage tank volume only becomes import for high solar fractions of 80% and higher. At constant generator temperatures and a collector mass flow of 30 kg m⁻² h⁻¹ the solar fraction drops by a maximum of 10 percentage points, if the specific storage volume is reduced from 50 liters m⁻² to 25 liters m⁻². For specific storage volumes above 0.06 m³m⁻², the solar fraction hardly changes (see figure 13).

As usual, the specific collector yield is highest for low solar fractions, i.e. for small collector surface areas. For the location Madrid/Spain it varies between 230 – 880 kWh m⁻² a⁻¹ (see figure 14).

In the following, the influence of storage tank volume, insulation thickness and heat exchanger size is evaluated for Case 2 conditions, i.e. improved control with varying generator temperatures. The solar fraction to the total heat demand is reduced by 2 percentage points for a typical insulation thickness of 10 cm compared to an ideal loss free storage tank (see figure 15). This corresponds to an additional auxiliary heating demand of 340 kWh or 9% more. Doubling the storage volume increases the solar fraction by one percentage point, which corresponds to a reduction of auxiliary heating energy

of 200 kWh or 5% less. The larger the storage tank, the more important good insulation quality. The specific collector energy delivered to the storage tank even drops if the insulation quality improves, as the storage tank is generally hotter. However, the energy delivered from the storage tank to the absorption chiller increases, so that in total the solar fraction improves.

The influence of the solar circuit heat exchanger was analysed by varying the transferred power UA per degree of temperature difference between primary and secondary circuit. The heat exchanger is usually dimensioned for the maximum power of the solar collector field. At a design mean operating temperature of the collectors of 85°C and an ambient air design temperature of 32°C the efficiency of the vacuum tube collectors chosen here is 67.5%, i.e. the collectors produce a maximum of 675 W m⁻² at full irradiance. For the given surface area of 31 m² and a set temperature difference across the heat exchanger of 3 K, this results in a transfer power of 7 kW K⁻¹. A reduction of transferred power from the solar circuit heat exchanger by 50% does not reduce the solar fraction at all.

Influence of dynamic building cooling loads

If a given cooling machine designed to cover the maximum load is used for different cooling load profiles, the influence of the specific load distribution and annual cooling energy demand can be clearly seen. The boundary conditions for the control were set to Case 2 conditions, i.e. a wet cooling tower, a low cold distribution temperature network of 6°C/12°C and variable generator inlet temperatures. The solar fraction was always at 80%. The office building with low internal loads and the main windows facing south requires 2 m² per kW solar thermal collector surface area (office 1). The same building with a different orientation to the east can be about 20% bigger in size to fit the 15 kW maximum cooling power. It has a 15% higher collector surface area and 15% less collector yield. If the building is orientated with the main window front to the west, the building surface area is only slightly higher than the south orientated building with a lower total cooling energy demand. The collector surface area is the same as for a south orientated building, which at lower operating hours means higher total costs.

The same building now dominated by internal loads (office 2) needs a collector surface area of 3.6 m² kW⁻¹, which is 80% times higher than for office 1, although the required maximum power is still only 15 kW. Due to the longer operating hours of the solar thermal cooling system, the specific collector yield is 22% higher at 784 kWh m⁻² a⁻¹ at the location Madrid/Spain, so that the solar thermal efficiency is 45% for solar cooling operation alone. If the office building with low internal loads is placed in Stuttgart/Germany with a more moderate climate, the collector yield drops to 324 kWh m⁻² a⁻¹ and the required surface area is 1.7 m² kW⁻¹ (see figure 16).

For the location Madrid, the collector surface area required to cover 1 MWh of cooling energy demand varies between 1.6 and 3.5 m² per MWh, depending on building orientation and control strategy chosen. The lower the cooling energy demand, the higher the required surface area per MWh. This is very clear for the building in Stuttgart with a low total energy demand of 4.7 MWh, where between 4.6 and 6.2 m² solar thermal collector surface area per MWh is necessary to cover the energy demand (see figure 17). The ratios between collector surface and cooling energy demand vary by about 25% for the same location and control strategy. In locations with lower annual irradiance such as Stuttgart, the required collector surface per MWh cooling energy demand is higher.

The storage volumes are comparable to typical solar thermal systems for warm water production and heating support and vary between 40 and 110 liter per square meter of collector surface area, depending on control strategy and cooling load file. They increase with cooling energy demand for a given location. In moderate climates with only occasional cooling energy demand, the storage volumes are generally higher (see figure 18).

Economical analysis

To plan and project energy systems such as solar cooling systems, economic considerations form the basis for decision making. The costs in energy economics can be divided in three categories: capital costs, which contain the initial investment including installation, operating costs for maintenance and system operation and the costs for energy and other material inputs into the system.

The analysis presented here is based on the annuity method, where all cash flows connected with the solar cooling installation are converted into a series of annual payments of equal amounts. The annuity a is obtained by first calculating the net present value of all costs occurring at different times

during the project, i.e. by discounting all costs to the time $t = 0$, when the investment takes place. The initial investment costs $P(t = 0)$ as well as further investments for component exchange in further years $P(t)$ result in a capital value CV of the investment, which is calculated using the inflation rate f and the discount or basic interest rate d . The discount rate chosen here was 4% and the inflation rate was set to 1.9%.

$$CV = \sum P(t) \frac{(1+f)^t}{(1+d)^t} \quad (1)$$

Annual expenses for maintenance and plant operation EX , which occur regularly during the lifetime N of the plant, are discounted to the present value by multiplication of the expenses with the present value factor PVF . Thermal chillers today can expect a lifetime of 20 years.

$$PVF(N, f, d) = \frac{1+f}{d-f} \left(1 - \left(\frac{1+f}{d-f} \right)^N \right) \quad (2)$$

In the case of solar cooling plants, no annual income is generated, so that the net present value NPV is simply obtained from the sum of discounted investment costs CV and the discounted annual expenses. It is here defined with a positive sign to obtain positive annuity values.

$$NPV = CV + EX \times PVF(N, f, d) \quad (3)$$

Annual expenses include the maintenance costs and the operating energy and water costs. For maintenance costs, some standards like VDI 2067 use 2% of the investment costs. Some chiller manufacturers calculate maintenance contracts with 1% of the investment costs. For large thermal chillers, some companies offer constant cost maintenance and repair contracts: the costs vary between 0.5% for large machines (up to 700 kW) up to 3% for smaller power. Repair contracts are even more expensive with 2% for larger machines up to 12% for a 100 kW machine. In the calculations shown here, 2% maintenance costs are used.

To obtain the annuity a as the annually occurring costs, the NPV is multiplied by a recovery factor r_f , which is calculated from a given discount rate d and the lifetime of the plant N . The cost per kWh of cold is the ratio of the annuity divided by the annual cooling energy produced.

$$a = NPV \times r_f(N, d) = NPV \times \frac{d(1+d)^N}{(1+d)^N - 1} \quad (4)$$

The investment costs for the cooling machines were obtained from an own market study (see figure 19). The costs are from manufacturers based in Germany and from a survey of the international energy agency (Henning, 2004). A regression through the data points was used to obtain the costs for the given power used in the calculations. With a discount rate of 4% and 1.9% inflation costs over a service life of 20 years, the annuity for the cooling machine alone was 1518 Euros per year.

In addition to the chiller investment costs, the annuity of the solar thermal system was calculated from the surface area dependent collector investment costs, the volume dependent storage costs and a fixed percentage of 12% for system technology and 5% mounting costs. Cost information for the solar thermal collectors and storage volumes were obtained from a German database for small collector systems, from the German funding program Solarthermie 2000 for flat plate collector surface areas above 100 m² and for vacuum tube collectors from different German distributors (see figure 20 and 21).

Maintenance costs and the operating costs for electrical pumps were set to 2%. Major unknowns are the system integration and installation costs, which depend a lot on the building situation, the connection to the auxiliary heating or cooling system, the type of cooling distribution system and so on. Due to the small number of installations, it is difficult to obtain reliable information about installation and system integration costs. Therefore, two simulation runs were done with different cost assumptions for installation and integration. The first simulations were done with very low installation costs of 5% of total investment plus 12% for system integration. A second round of simulations is based on 25% installation and 20% system integration costs.

The total costs per MWh of cold produced C_{total} are obtained by summing the chiller cost $C_{chiller}$ to the solar costs C_{solar} , the auxiliary heating costs C_{aux} and the costs for the cooling water production

$C_{cooling}$. The costs for heating have to be divided by the average COP of the system to refer the cost per MWh heat to the cold production and multiplied by the solar fraction s_f for the respective contributions of solar and auxiliary heating. For the cooling water, the costs per MWh of cooling water were taken from literature (Gassel, 2004) and referred to the MWh of cold by multiplication with $(1 + \frac{1}{COP})$ for removing the evaporator heat (factor 1) and the generator heat with a factor $\frac{1}{COP}$.

$$C_{total} = C_{chiller} + \frac{s_f C_{solar}}{COP} + \frac{(1 - s_f) C_{aux}}{COP} + C_{cooling} \left(1 + \frac{1}{COP}\right) \quad (5)$$

A value for $C_{cooling}$ of 9 € per MWh cooling water was used and the auxiliary heating costs $C_{heating}$ were set to 50 € per MWh heat.

The chosen system technology (dry or wet chiller, low or high temperature distribution system, control strategy) influences the costs only slightly (7% difference between the options), if the operating hours are low (such as in the office 1 example with low internal loads, see figure 23). If the operating hours increase, the advantage of improving the control strategy (Case 2) or increasing the temperature levels of the cooling distribution system (Case 3) become more pronounced (16% difference between the different cases, see figure 24).

For very low operating hours such as the office building in the Stuttgart climate with only 313 full load hours, the costs are between 640 and 700 € MWh⁻¹, 60% of which are due to the chiller investment costs only (see figure 22).

The calculated solar thermal system costs were between 85 € MWh⁻¹ and 258 € MWh⁻¹ for solar cooling applications, depending on the operating hours and the location. They go down as far as 76 € MWh⁻¹ for the office in Madrid with high internal loads and a high temperature cooling distribution system. These costs are getting close to economic operation compared with fossil fuel heating supply. The main dimensioning results for the buildings with a good control strategy and a low temperature fan coil distribution system (Case 2) are summarized in table 5 and 6. The total costs per MWh of cold produced by the thermal chillers are given in table 7.

If the system integration and mounting costs are assumed to be 45% of total investment costs instead of 17%, the costs per MWh of cold are in the range of 300 – 390 € MWh⁻¹ for the office in Madrid with low internal loads and 200 € MWh⁻¹ for the best case of the office with longer operating hours (see figure 25).

By comparison, Schölkopf (2004) calculated the cost of conventional cooling systems for an energy efficient office building in Germany with 180 € per MWh. 17% of the cost were for the electricity consumption of the chiller. The total annual cooling energy demand for the 1094 m² building was 31 kWh m⁻²a⁻¹. Own comparative calculations for a 100 kW thermal cooling project showed that the compression chiller system costs without cold distribution in the building were between 110 and 140 € per MWh.

Henning (2004) also investigated the costs of solar cooling systems compared to conventional technology. The additional costs for the solar cooling system per MWh of saved primary energy were between 44 € per MWh in Madrid and 77 € per MWh in Freiburg for large hotels. It is clear that solar cooling systems can only become economically viable, if both the solar thermal and the absorption chiller costs decrease. This can be partly achieved by increasing the operation hours of the solar thermal system and thus the solar thermal efficiency by using the collectors also for warm water production or heating support.

Conclusions

In the work the design, performance and economics of solar thermal absorption chiller systems were analysed. Absorption chillers were modeled under partial load conditions by solving the steady state energy and mass balance equations for each time step. The calculated cooling power and coefficient of performance fit the experimental data better than a constant characteristic equation. The chiller model was integrated into a complete simulation model of a solar thermal plant with storage, chiller and auxiliary heating system. Different cooling load files with a dominance on either external or internal loads for different building orientations and locations were created to evaluate the influence of the special load time series for a given cooling power. The investigation showed that to achieve a given solar fraction of the total heat demand requires largely different collector surfaces and storage volumes,

depending on the characteristics of the building load file and the chosen system technology and control strategy. To achieve a solar fraction of 80% at the location Madrid, the required collector surface area is above $3 \text{ m}^2 \text{ kW}^{-1}$, if the generator is operated at constant high temperature of 85°C and the solar thermal system operates under low flow conditions. In this case, it is very recommendable to increase the collector field mass flow, so that temperature levels cannot rise too much. Doubling of mass flow decreases the required collector surface area and thus solar thermal system costs by 30%.

For buildings with the same maximum cooling load, but different load time series, the required surface area varies by a factor 2 to obtain the same solar fraction. The influence of building orientation with the same internal load structure is about 15%. More important are different internal loads, which can increase the required collector surface area by nearly a factor 2. The best solar thermal efficiency was 45% for high full load hours of nearly 2000 hours. For the location Madrid, 80% solar fraction are possible for surface areas between $2 - 4 \text{ m}^2$ per kW cooling power, the high values occurring for larger full load hours. For each MWh of cooling energy demand, between 1.6 and 3.5 m^2 collector surface are required for the Spanish site and between 4.6 and 6.2 m^2 for the German installation. The total system costs for commercially available solar cooling systems are between $180 - 270 \text{ € MWh}^{-1}$, again depending on the cooling load file and the chosen control strategy. The total costs are dominated by the costs for the solar thermal system and the chiller itself. For a more moderate climate with low cooling energy demand, the costs can rise as high as 680 € MWh^{-1} . The work shows that dynamic system simulations are necessary to determine the correct solar thermal system size and to reach a given solar fraction of the total energy requirement.

Acknowledgements

The authors like to thank our colleagues Martin Huber, who provided the building load files using TRNSYS, and Juergen Schumacher, who supported the solar cooling modelling work in INSEL.

References

- [1] Albers, J., Ziegler, F., Analysis of the part load behaviour of sorption chillers with thermally driven solution pumps, Proceedings of the 21st IIR International Congress of Refrigeration, August 17-22, International Institute of Refrigeration (IIR), Washington D.C., USA, ISBN 2-913149-32-4, 2003
- [2] Atmaca, I., Yigit, A., Simulation of solar-powered absorption cooling system, Renewable Energy 28, 2003
- [3] Engler, M., Grossmann, G., Hellmann, H.-M., Comparative simulation and investigation of ammonia-water: absorption cycles for heat pump applications, Int. J. Refrig., Vol 20, No 7, pp 504-516, 1997
- [4] EAW, Absorptionskälteanlage Wegracal SE 15 – Technische Beschreibung (Absorption Chiller Wegracal SE 15 – technical description). Company product information. EAW Energieanlagenbau GmbH, Germany, 2003
- [5] Florides, G.A., Kalogirou, S.A., Tassou, S.A., Wrobel, L.C., Modelling, simulation and warming impact assessment of a domestic-size absorption solar cooling system, Applied Thermal Engineering, Vol 22, No 12, 2002
- [6] Gassel, A., Kraft-Wärme-Kälte-Kopplung und solare Klimatisierung, Habilitationsschrift TU Dresden, 2004
- [7] Grossmann, G., Solar powered systems for cooling, dehumidification and air conditioning, Solar Energy Vol. 72, pp53-62, 2002
- [8] Henning, H.-M. Solar-assisted air-conditioning in buildings – a handbook for planners, Springer-Verlag 2004, ISBN 3-211-00647-8

- [9] Henning, H.-M., Solare Klimatisierung - Stand der Entwicklung Fraunhofer-Institut für Solare Energiesysteme ISE Tagung Solares Kühlen, Wirtschaftskammer Österreich, Wien, 7.5.2004
- [10] INSEL 7.0 Block reference manual, www.inseldi.com
- [11] Jakob, U., Eicker, U., Taki, A.H., Cook, M.J., Development of an optimised solar driven Diffusion-Absorption Cooling Machine, Proceedings of the ISES Solar World Congress 2003, June 16-19, International Solar Energy Society (ISES), Göteborg, Sweden, ISBN 91-631-4740-8, 2003
- [12] Jakob, U., Investigations into Solar Powered Diffusion-Absorption Cooling Machines, PhD Thesis, De Montfort University Leicester, 2005
- [13] Kim, D.S., Machielsen, C.H.M., Evaluation of air-cooled solar absorption cooling systems, ISHPC '02, Proceedings of the International Sorption Heat Pump Conference, Shanghai, China, September 24-27, 2002
- [14] Kim, D.S., Wang, L., Machielsen, C.H.M., Dynamic modelling of a small-scale NH₃/H₂O absorption chiller, Proceedings of the 21st IIR International Congress of Refrigeration, August 17-22, International Institute of Refrigeration (IIR), Washington D.C., USA, ISBN 2-913149-32-4, 2003
- [15] Mendes, L.F, Collares-Pereira, M., Ziegler, F. , Supply of cooling and heating with solar assisted heat pumps: an energetic approach", Int. J. Refrig. Vol 21, No.2, pp 116-125, 1998
- [16] Schumacher, J. Digitale Simulation regenerativer elektrischer Energieversorgungssysteme, Dissertation Universität Oldenburg, 1991 www.inseldi.com
- [17] Schweigler, C., Storckenmaier, F., Ziegler, F, Die charakteristische Gleichung von Sorptionskälteanlagen, Proceedings of the 26th Deutsche Klima-Kälte-Tagung, Berlin, Germany, 1999
- [18] Schoelkopf, W., Kuckelkorn, J., Verwaltungs- und Bürogebäude – Nutzerverhalten und interne Wärmequellen, OTTI Kolleg Klimatisierung von Büro- und Verwaltungsgebäuden, Regensburg 9/2004
- [19] Yasuo Takagi, Tadashi Nakamaru and Yoshihiko Nishitani, an absorption chiller model for HVAC-SIM+, Toshiba corporation, proceedings of the international building performance simulation association, 1999
- [20] Tommy, H.J.M. (1994), Simulation of a PV-Diesel Generator Hybrid System and Investment Analysis: Case Study of a Mountain Hostel, Master Thesis, Renewable Energy Group, Department of Physics, Carl von Ossietzky University Oldenburg, Germany
- [21] Wardono, B., Nelson, R.M., Simulation of a double effect LiBr/H₂O Absorption Cooling System, ASHRAE Journal pp 32-38, October 1996
- [22] Willers, E., Neveu, P., Groll, M., Kulick, C., Meunier, F., Mostofizadeh, C., Wierse, M., Dynamic modelling of a liquid absorption system, ISHPC '99, Proceedings of the International Sorption Heat Pump Conference, Munich, Germany, March 24-26, 1999
- [23] Ziegler, F. , Sorptionswärmepumpen, Forschungsberichte des Deutschen Kälte- und Klimatechnischen Vereins Nr. 57, Stuttgart, ISBN 3-932715-60-8, 1998

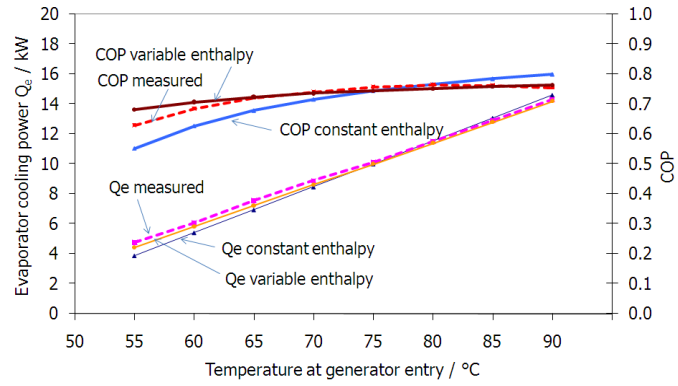


Figure 1: Measured and simulated cooling power as a function of generator entry temperature for a 10 kW absorption chiller.

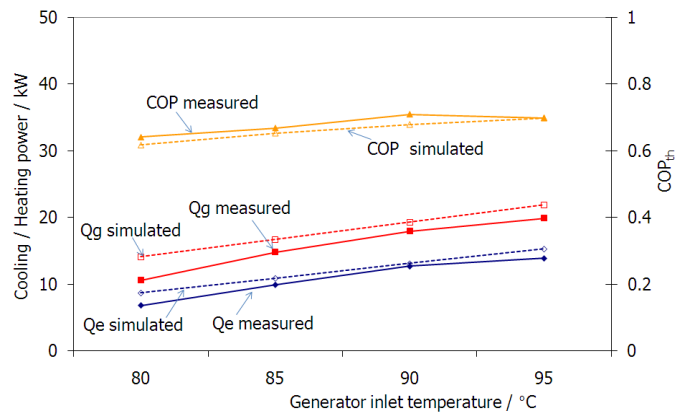


Figure 2: Power and COP of a 15 kW cooling machine as a function of generator temperature.

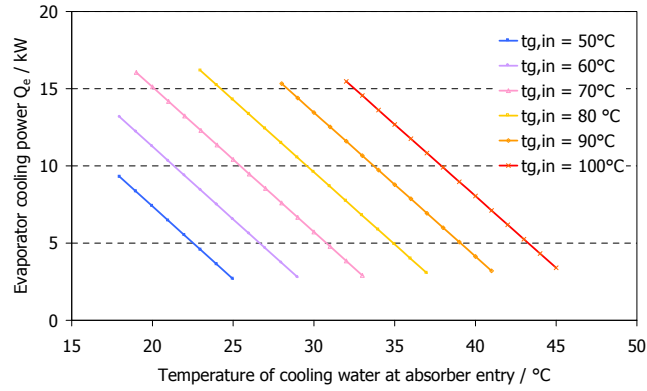


Figure 3: Simulated cooling power as a function of cooling water temperature for a market available 15 kW absorption chiller.

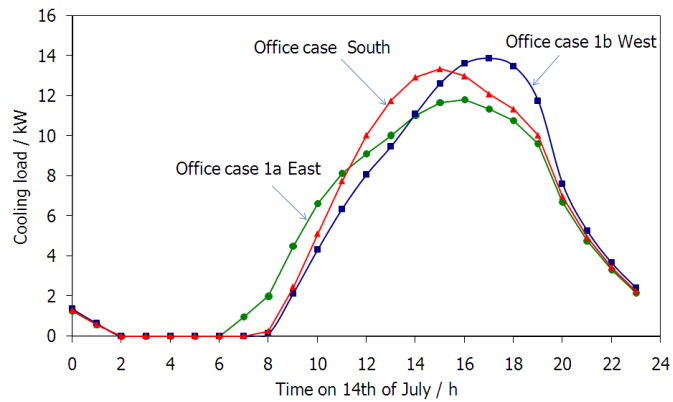


Figure 4: Daily cooling loads of a small office building with the main window front facing east, south or west.

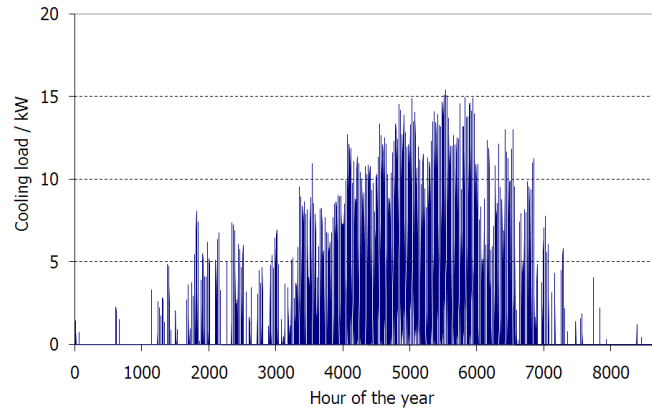


Figure 5: Office building dominated by external loads located in Madrid, Spain (office 1).

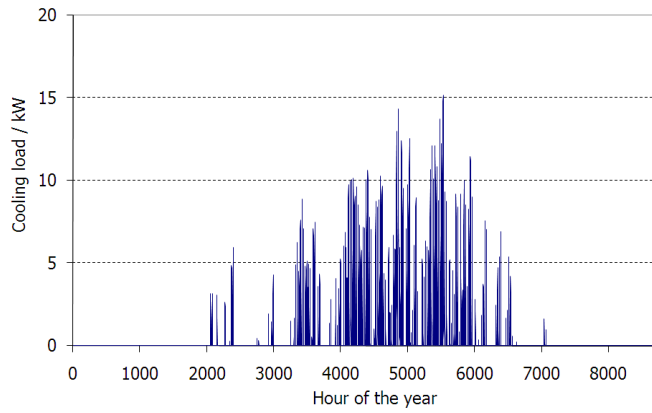


Figure 6: Office building dominated by external loads at the location Stuttgart/Germany (office 3).

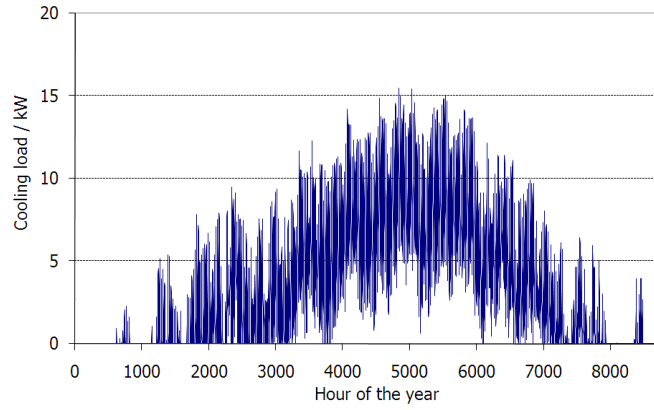


Figure 7: Office building with high internal loads and good sun protection (office 2) at the location Madrid.

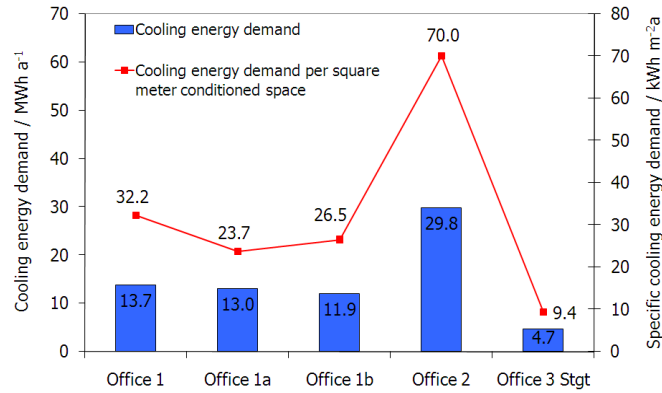


Figure 8: Specific and total annual cooling energy demand for the office building with different orientations and locations and dominated either by external (case 1) or internal (case 2) loads.

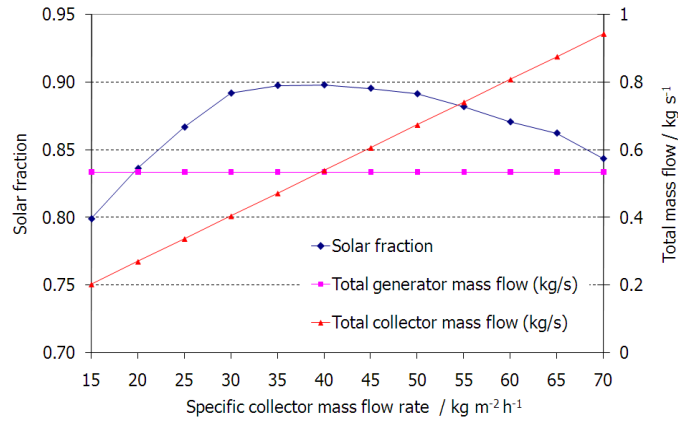


Figure 9: Influence of collector mass flow on solar fraction for constant generator inlet temperature.

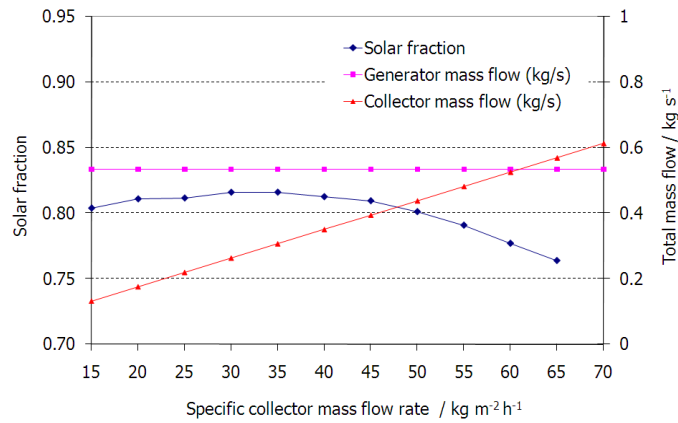


Figure 10: Influence of collector mass flow on solar fraction for variable generator inlet temperature.

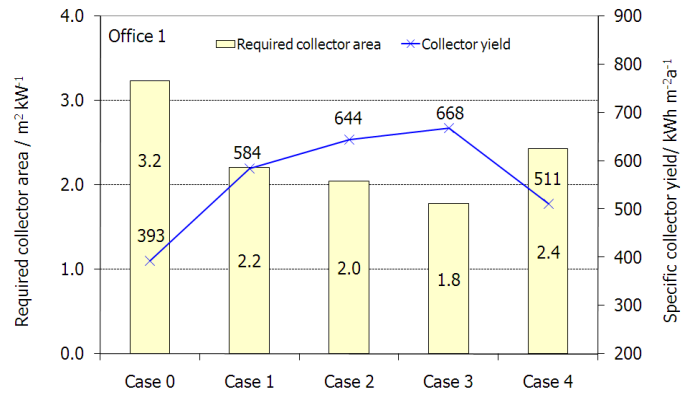


Figure 11: Required collector area per kW cooling power to achieve 80% solar fraction for different generator and evaporator inlet temperatures applied to the office case 1.

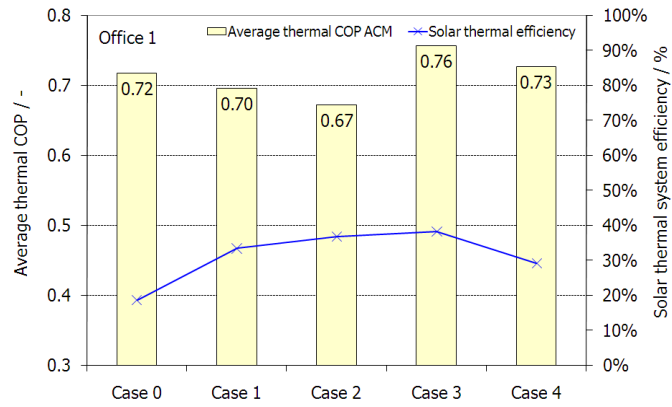


Figure 12: Average annual COP and solar thermal collector efficiency for different operation modes.

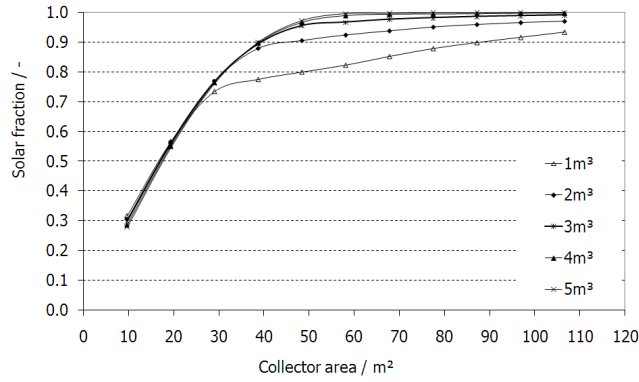


Figure 13: Solar fraction as a function of collector surface area for a 15 kW solar cooling system with constant generator temperatures (Case 1).

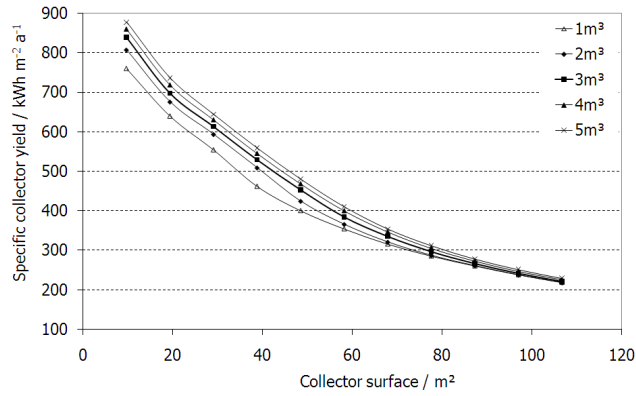


Figure 14: Collector yield as a function of collector surface area for constant generator temperature (Case 1). The storage volume is varied from 1 to 5 m³.

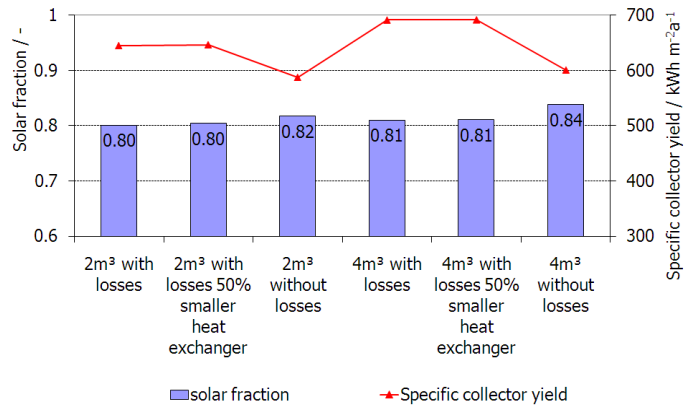


Figure 15: Influence of storage tank insulation and heat exchanger size on solar fraction and specific collector yield.

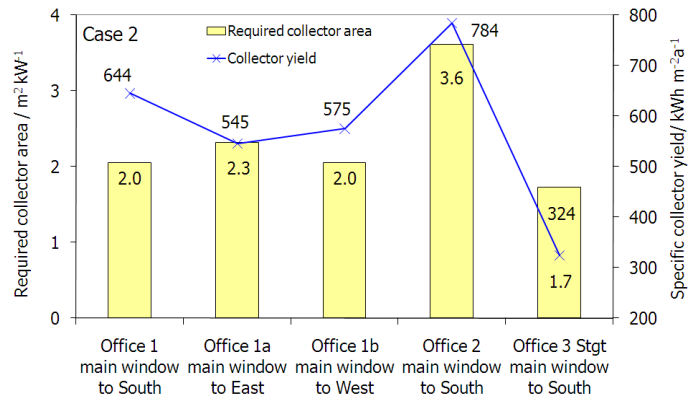


Figure 16: Correlation between required collector area and maximum building cooling load.

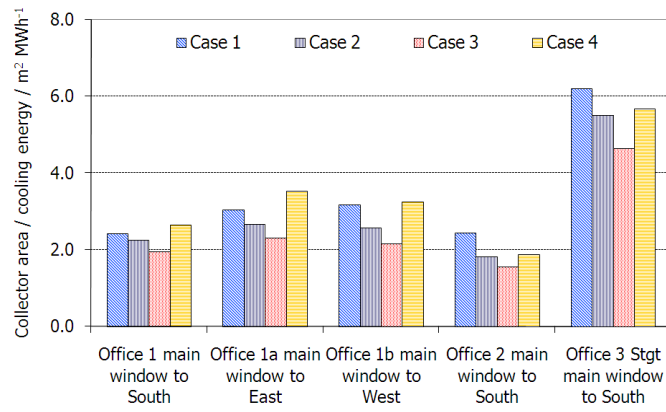


Figure 17: Required collector surface area as a function of the cooling energy requirement of office buildings. All buildings are located in Madrid/Spain apart from office 3.

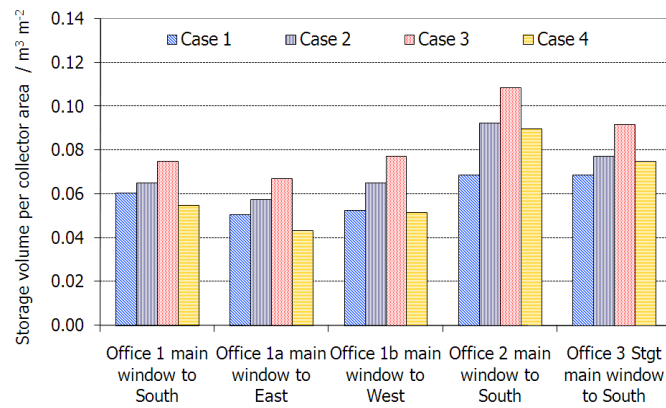


Figure 18: Storage volume per square meter of collector surface for different building load files.

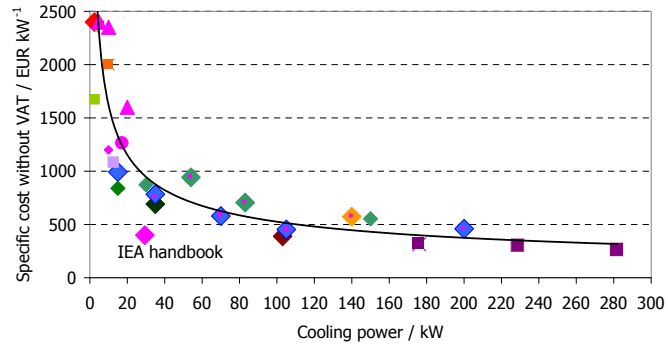


Figure 19: Investment costs of low power thermal absorption chillers.

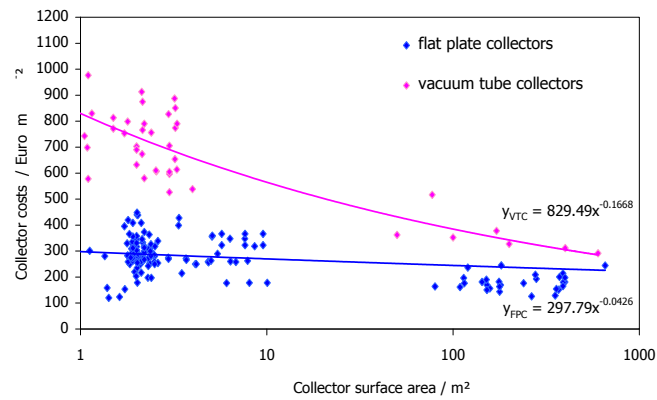


Figure 20: Specific collector costs without VAT as a function of size of the installation.

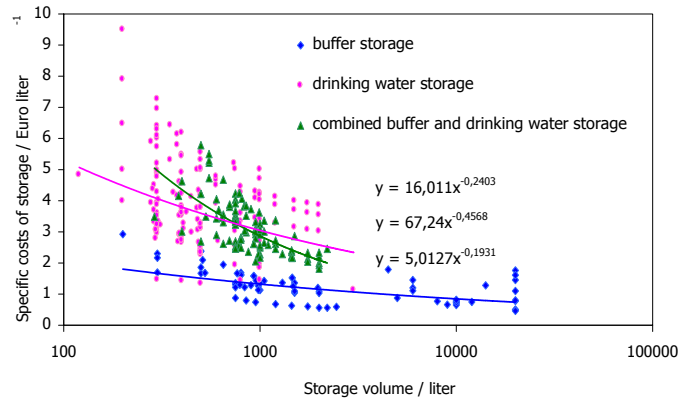


Figure 21: Costs for different storage tank systems.

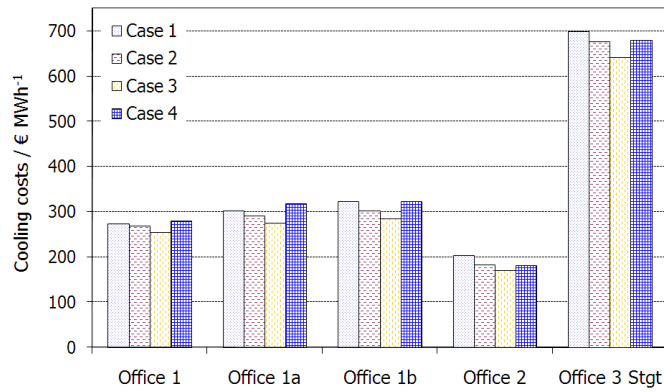


Figure 22: Cooling costs for different load situations and system technologies for the locations Madrid and Stuttgart.

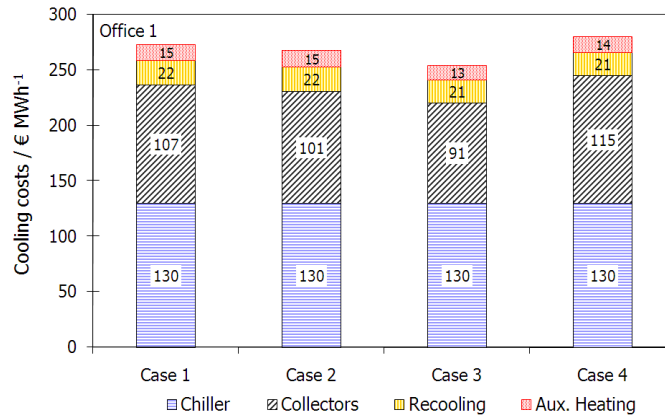


Figure 23: Cooling costs per MWh of cold for different system technology options and control strategies.

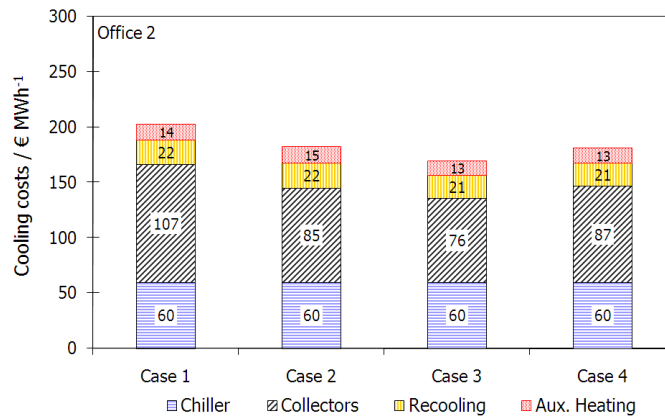


Figure 24: Cooling costs for different operation strategies and cooling distribution systems for the office with high internal loads.

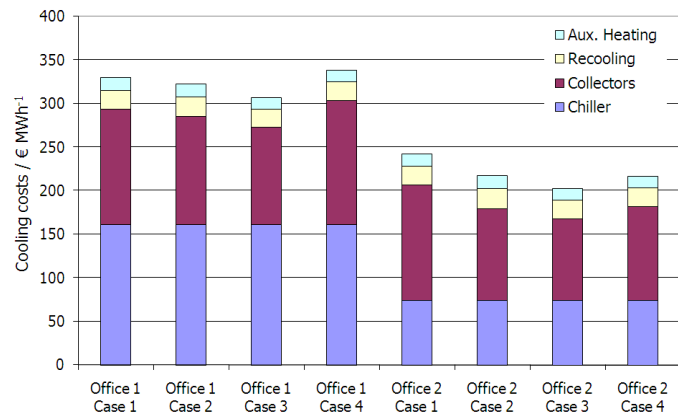


Figure 25: Cost distribution for a solar thermal absorption chiller system with mounting and integration costs of 45% of total investment cost.

Building type	Internal load	Full load hours
	/ W m ⁻²	/ h
Office 1 Madrid	4	913
Office 1a Madrid	4	866
Office 1b Madrid	4	793
Office 2 Madrid	20	1986
Office 3 Stuttgart	4	313

Table 1: Internal loads and full load hours for the building in different locations.

Building Case	Window surface fraction / %				Shading fraction / %			
	North	South	East	West	North	South	East	West
O1 Madrid/ O3 Stuttgart	39	39	11	11	0	0	0	0
O1a	39	11	39	11	0	0	0	0
O1b	39	11	11	39	0	0	0	0
O2	39	39	11	11	90	90	90	90

Table 2: Window size and shading fractions for cooling load calculations.

Building type	Surface	Volume
	/ m ²	/ m ³
Office 1	425	1275
Office 1a	550	1650
Office 1b	450	1350
Office 2	450	1350
Office 3 Stuttgart	500	1500

Table 3: Cooling power and full load hours for the building types in different locations.

Cases	Cooling tower type	Cold distribution		Generator inlet	
		6°C	15°C	85°C	70-95°C
		/	/	Const	Variable
		12°C	21°C		
Case 0	wet	x		x	
Case 1	wet	x		x	
Case 2	wet	x			x
Case 3	wet		x		x
Case 4	dry		x		x

Table 4: Summary of boundary conditions for different simulation runs. Case 0 and Case 1 both operate at constant generator temperature, but in Case 0 the solar thermal system operates at low flow conditions.

Case	Cooling load file	Chiller power / kW	Collector area / m ²	Storage volume / m ³	Solar yield / kWh m ⁻²	Average COP –
O1	office 1	15	31	2	644	0.67
O2	office 2	15	54	5	784	0.67
O3	office 3	15	25	2	324	0.64

Table 5: Summary of design values for the office with variable control strategy (Case 2). Office 1 and 2 are located in Madrid, office 3 in Stuttgart.

Case	Cooling energy demand / MWh	Collector surface per MWh / m ² MWh ⁻¹	Collector surface per kW / m ² kW ⁻¹	Storage volume per surface / m ³ m ⁻²	Solar thermal efficiency / %
O1	13.7	2.2	2.0	0.07	37
O2	29.8	1.8	3.6	0.09	45
O3	4.7	5.5	1.7	0.08	26

Table 6: Summary of energy performance data.

Case	Solar investment €	Total investment €	Chiller cost $C_{chiller}$ € MWh _{cold} ⁻¹	Solar cost C_{solar} € MWh _{heat} ⁻¹	Total cost C_{total} € MWh _{cold} ⁻¹
O1	14260	32490	130	101	268
O2	22400	40630	60	85	183
O3	12140	30370	378	258	676

Table 7: Costs for solar thermal cooling systems